

MODELING MULTIFRACTALITY OF THE SOLAR WIND

WIESŁAW M. MACEK

*Faculty of Mathematics and Natural Sciences. College of Sciences, Cardinal Stefan Wyszyński University, Dewajtis 5, 01-815 Warszawa, Poland; Space Research Centre, Polish Academy of Sciences, Bartycka 18 A, 00-716 Warszawa, Poland
(E-mail: macek@cbk.waw.pl)*

(Received: 27 October 2005; Accepted in final form: 12 April 2006)

Abstract. The question of multifractality is of great importance because it allows us to investigate interplanetary hydromagnetic turbulence. The multifractal spectrum has been investigated with Voyager (magnetic field) data in the outer heliosphere and with Helios (plasma) data in the inner heliosphere. We use the Grassberger and Procaccia method that allows calculation of the generalized dimensions of the solar wind attractor in the phase space directly from the cleaned experimental signal. We analyze time series of plasma parameters of the low-speed streams of the solar wind measured *in situ* by Helios in the inner heliosphere. The resulting spectrum of dimensions shows a multifractal structure of the solar wind attractor. In order to quantify that multifractality, we use a simple analytical model of the dynamical system. Namely, we consider the generalized self-similar baker's map with two parameters describing uniform compression and natural invariant measure on the attractor of the system. The action of this map exhibits stretching and folding properties leading to sensitive dependence on initial conditions. The obtained solar wind singularity spectrum is consistent with that for the multifractal measure on the weighted baker's map.

Keywords: time series analysis, solar wind plasma, fractals, chaotic dynamics

1. Introduction

The question of multifractality is of great importance also for the solar wind community, because it allows us to investigate the nature of interplanetary hydromagnetic turbulence (e.g., Marsch and Tu, 1997; Bruno *et al.*, 2001). Starting from Richardson's version of turbulence, many authors try to recover the observed scaling exponents using various models of the turbulence cascade for the dissipation rate. In particular, the multifractal spectrum was investigated with Voyager (magnetic field) data in the outer heliosphere (e.g., Burlaga, 1991, 2001) and with Helios (plasma) data in the inner heliosphere (e.g., Marsch *et al.*, 1996).

A direct determination of the multifractal spectrum from the data is known to be a difficult problem. Indication for a chaotic attractor in the slow solar wind has been given by Macek (1998) and Macek and Redaelli (2000). In particular, Macek (1998) has calculated the correlation dimension of the reconstructed attractor in the solar wind and has provided tests for this measure of *complexity* including statistical surrogate data tests (Theiler *et al.*, 1992). Further, Macek and Redaelli (2000) have

shown that the Kolmogorov entropy of the attractor is *positive* and finite, as it holds for a *chaotic* system.

We have extended our previous results on the dimensional time series analysis (Macek, 1998). Namely, we have applied the technique that allows a realistic calculation of the generalized dimensions of the solar wind flow directly from the cleaned experimental signal by using the Grassberger and Procaccia (1983) method. The resulting spectrum of dimensions shows the multifractal structure of the solar wind in the inner heliosphere (Macek *et al.*, 2005, 2006). Using a short data sample, we first demonstrate the influence of noise on these results and show that noise can efficiently be reduced by a singular-value decomposition filter (Macek, 2002, 2003). Using a longer sample we have shown that the multifractal spectrum of the solar wind attractor reconstructed in the phase space is consistent with that for the multifractal measure on the self-similar weighted baker's map (Macek *et al.*, 2005) and, in particular, with the weighted Cantor set (Macek *et al.*, 2006).

2. Solar Wind Data

In this paper, we analyze the Helios 2 data using plasma parameters measured *in situ* in the inner heliosphere (Schwenn, 1990). The X -velocity (mainly radial) component of the plasma flow, v , has been investigated by Macek (1998) and Macek and Redaelli (2000). However, it is known that various disturbances are superimposed on the overall structure of the solar wind, including mainly Alfvén waves. Therefore, in this paper we take into account Alfvénic fluctuations of the flow. Namely, Macek *et al.* (2005) analyze the radial (X -) component of one of the Elsässer variables, $x = z_+$, representing Alfvénic fluctuations propagating outward from the Sun. We have $z_+ = v + v_A$ for the unperturbed magnetic field B_0 pointing to the Sun and $z_+ = v - v_A$ for B_0 pointing away from the Sun, where $v_A = B/(\mu_0\rho)^{1/2}$ is the Alfvénic velocity calculated from the experimental data: the radial component of the magnetic field of the plasma B and the mass density ρ (μ_0 is the permeability of free space). Assuming absence of radial evolution, we have merged two selected time intervals separated by about 0.5 AU as observed by the Helios 2 spacecraft in 1977 (i) from 116:00 to 121:21 (day:hour) at distances 0.30–0.34 AU and (ii) from 348:00 to 357:00 at 0.82–0.88 AU from the Sun. These raw data of v and v_A , $N = 26,163$ points, with sampling time of $\Delta t = 40.5$ s are shown in Figure 1a, taken from Macek *et al.* (2005). The first sample of $N = 10,644$ points have been investigated by Macek *et al.* (2006).

In Macek *et al.* (2005) slow trends were subtracted from the original data $v(t_i)$ and $v_A(t_i)$, where $i = 1, \dots, N$. The data with the initial several-percent noise level were (eightfold) smoothed (replacing each data point with the average of itself and its two nearest neighbors). Next, the data have been filtered using a method of singular-value decomposition analysis described by Albano *et al.* (1988). As argued by Macek (1998) we use five principal eigenvalues. The detrended and filtered data

TABLE I
Characteristics of the solar wind filtered data, z_+ .

Skewness (κ_3)	0.59
Kurtosis (κ_4)	0.37
Dominant frequency	2.5×10^{-5} Hz
Autocorrelation time (t_a)	7.05×10^3 s
Capacity dimension (D_0)	3.87 ± 0.10
Information dimension (D_1)	3.26 ± 0.08
Correlation dimension (D_2)	3.35 ± 0.06

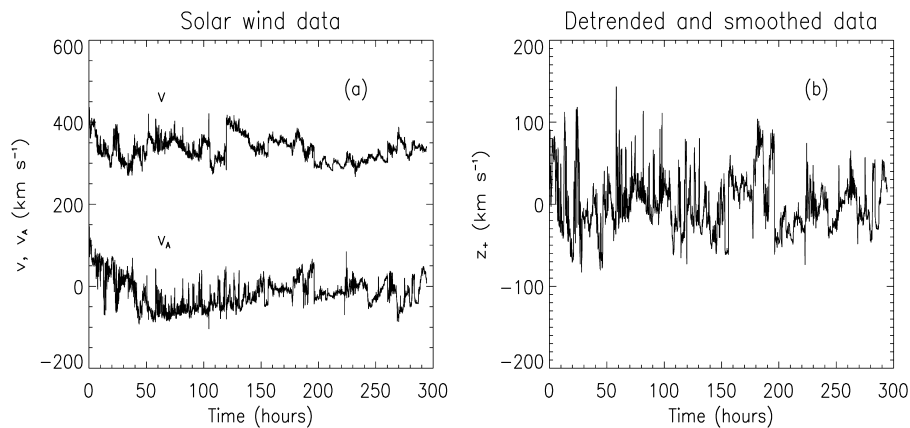


Figure 1. (a) The raw data of the radial flow velocity with Alfvénic velocity, v and v_A , observed by the Helios 2 spacecraft in 1977 from 116:00 to 121:21 (day:hour) at a distance of 0.3 AU and from 348:00 to 357:00 at a distance of 0.9 AU from the Sun. (b) The Elsässer variable $z_+ = v \pm v_A$ for B_0 pointing to/away from the Sun for the detrended and filtered data using singular-value decomposition with the five largest eigenvalues.

for the radial component of the Elsässer variable $x = z_+$ are shown in Figure 1b also taken from Macek *et al.* (2005).

Table I summarizes selected calculated characteristics of the detrended data cleaned by using the singular-value decomposition filter (see, Macek *et al.*, 2005). The probability distributions are clearly non-Gaussian. We have a large skewness of ~ 0.59 (as compared with its normal standard deviation 0.02) and a large kurtosis of 0.37, the latter was small for the analysis with no magnetic field (cf. Macek, 1998). We choose a time delay $\tau = 174 \Delta t$, equal to the autocorrelation time t_a where the autocorrelation function decreases to $1/e$ (cf. Macek, 2003, Figure 1b). This makes certain that $x(t)$ and $x(t + \tau)$ are at least linearly time independent (e.g., Ott, 1993).

3. Generalized Dimensions

The generalized dimensions of attractors are important characteristics of *complex* dynamical systems (e.g., Grassberger, 1983; Hentschel and Procaccia, 1983). Since these dimensions are related to frequencies with which typical orbits in the phase space visit different regions of the attractors, they provide information about dynamics of the systems (Ott, 1993). More precisely, one may distinguish a probability measure from its geometrical support, which may or may not have fractal geometry. Then, if the measure has different fractal dimensions on different parts of the support, the measure is multifractal (Mandelbrot, 1989).

Using our time series of equally spaced, detrended, and cleaned data, we construct many vectors $\mathbf{X}(t_i) = [x(t_i), x(t_i + \tau), \dots, x(t_i + (m - 1)\tau)]$ in the embedding phase space of dimension m , where $i = 1, \dots, n$ with $n = N - (m - 1)\tau$. Then, in this space we construct a large number $M(r)$ of hyperspheres of radius r which cover the presumed attractor. If p_j is the probability measure that a point from a time series falls in a typical j th hypersphere, using the q -order function $I_q(r) = \sum (p_j)^q$, $j = 1, \dots, M$, the q -order generalized dimension D_q is given, e. g., by Ott (1993)

$$\tau(q) \equiv (q - 1)D_q = \lim_{r \rightarrow 0} \frac{\ln I_q(r)}{\ln r}, \quad (1)$$

where q is a continuous index, $-\infty < q < \infty$. We see from Equation (1) that the larger q is, the more strongly the higher-probability spheres (visited more frequently by a trajectory) weighted in the sum for $I_q(r)$. Only if $q = 0$, all the hyperspheres are counted equally, $I_0 = M$, and we recover the box-counting dimension, $D_0 = \lim_{r \rightarrow 0} [\ln M(r) / \ln(1/r)]$. The limit $q \rightarrow 1$ provides the information dimension, $D_1 = \lim_{r \rightarrow 0} [\sum (p_j \ln p_j) / \ln r]$.

Writing $I_q(r) = \sum p_j (p_j)^{q-1}$ as a weighted average $\langle (p_j)^{q-1} \rangle$, one can associate bulk with the generalized average probability per hypersphere $\mu = \langle (p_j)^{q-1} \rangle^{1/(q-1)}$, and identify D_q as a scaling of bulk with size, $\mu \propto r^{D_q}$. Since the data cannot constrain well the capacity dimension D_0 , we look for higher-order dimensions, which quantify the multifractality of the probability measure on the attractor. For example, the limit $q \rightarrow 1$ leads to a geometrical average, and the information dimension is $D_1 \approx \langle \ln p_j \rangle / \ln r$. For $q = 2$, the generalized average is the ordinary arithmetic average, with the standard correlation dimension $D_2 \approx \ln \langle p_j \rangle / \ln r$, and for $q = 3$ it is a root-mean-square average. In practice, the probability for a j th hypersphere of radius r is the ratio of the number of distances from a chosen vector $\mathbf{X}(t_j)$ that are less than r to the total number of distances between that vector and other vectors

$$p_j \simeq \frac{1}{n - 2n_c - 1} \sum_{i=n_c+1}^n \theta(r - |\mathbf{X}(t_i) - \mathbf{X}(t_j)|) \quad (2)$$

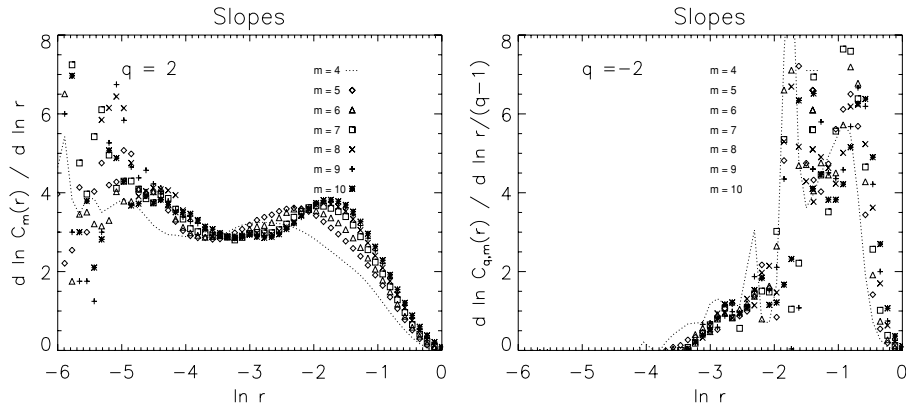


Figure 2. The slopes $D_{q,m}(r) = d[\ln C_{q,m}(r)]/d(\ln r)/(q - 1)$ of the generalized correlation sum $C_{q,m}(r)$ vs. $\ln r$ (normalized) obtained for detrended and filtered data are shown for various embedding dimensions m for (a) $q = 2$ and (b) $q = -2$.

with $\theta(x)$ being the unit step function, and n_c is the Theiler's (1986) correction ($n_c = 4$ is chosen). Finally, for a given m , $I_q(r)$ is taken to be equal to the generalized q -point correlation sum (Grassberger and Procaccia, 1983)

$$C_{q,m}(r) = \frac{1}{n_{\text{ref}}} \sum_{j=1}^{n_{\text{ref}}} (p_j)^{q-1}, \tag{3}$$

where n_{ref} is the number of reference vectors ($n_{\text{ref}} = 5,000$ is taken). For large dimensions m and small distances r in the scaling region it can be argued that $C_{q,m}(r) \propto r^{\tau(q)}$, where $\tau(q)$ is an approximation of the ideal limit $r \rightarrow 0$ in Equation (1) for a given q (Grassberger and Procaccia, 1983).

4. Dimensions and Multifractality

We first calculate the natural logarithm of the generalized correlation sum $C_{q,m}(r)$ of Equation (3) versus $\ln r$ (normalized) for various q and embedding dimensions: $m = 4$ (dotted curve), $m = 5$ (diamonds), $m = 6$ (triangles), $m = 7$ (squares), $m = 8$ (crosses), $m = 9$ (pluses), and $m = 10$ (stars) (cf. Macek, 2002, Figure 2). We have verified that for $q > 0$ the slopes $D_{q,m}(r) = d[\ln C_{q,m}(r)]/d(\ln r)/(q - 1)$ in the scaling region of $\ln r$ do not change substantially with the number of points used, providing that the dimension of the attractor is well below $2 \log_{10} N \approx 9$, for $N = 26,163$ (Eckmann and Ruelle, 1992). The results obtained using the moving average filter and singular-value decomposition linear filter for standard $q = 2$, as taken from Macek *et al.* (2005, Figure 2), and in addition $q = -2$ are presented in Figure 2a and b, correspondingly, while those obtained for somewhat shorter

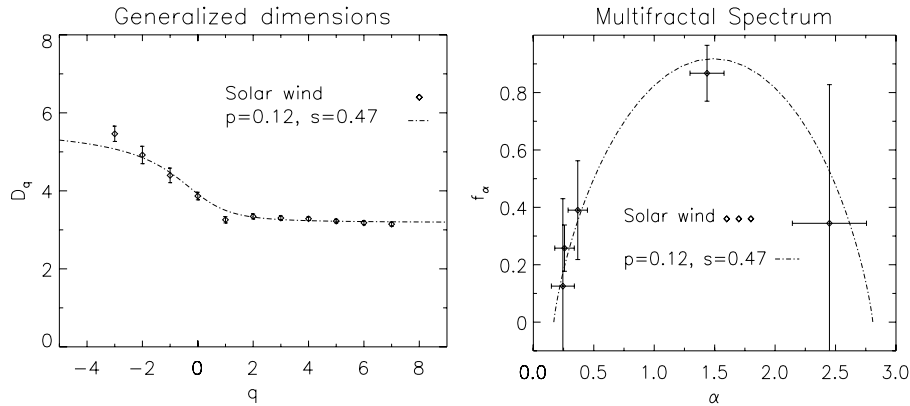


Figure 3. (a) The generalized dimensions D_q in Equation (1) as a function of q . The correlation dimension is $D_2 = 3.4 \pm 0.1$ (see Table I). The values of $D_q + 3$ are calculated analytically for the weighted baker's map with $p = 0.12$ and $s = 0.47$ (dashed-dotted line). (b) The singularity spectrum $f(\alpha)$ as a function of α . The values of $f(\alpha)$ projected onto one axis for the weighted baker's map with the same parameters (dashed-dotted line).

samples ($N = 4,514$) have been discussed by Macek (1998) and by Macek and Redaelli (2000), using the nonlinear Schreiber filters.

Usually in all these cases for $q > 0$ we have clear plateaus over a decade; the slopes of $C_{q,m}(r)$ saturate for $m > 5$ and the average slope for $6 \leq m \leq 10$ is taken as $\tau = (q - 1)D_q$. In particular, for the standard ($q = 2$) correlation sum we have obtained an average of $D_2 = 3.35 \pm 0.06$. The obtained measures of the attractor have been subjected to the surrogate data test (Theiler *et al.*, 1992). As has been demonstrated by Macek (1998), if the original data are indeed deterministic, analysis of these surrogate data will provide values that are statistically distinct from those derived for the original data. The results of this test are consistent with the attractor of low dimensions.

Next, the generalized dimensions D_q in Equation (1) as a function of q with the statistical errors of the average slopes (obtained using weighted least-squares fitting) over the scaling range are shown in Figure 3a (cf. Macek *et al.*, 2005, Figure 3). In addition, here in Figure 3b we show the singularity spectrum $f(\alpha)$, which follows from Equation (1) by using Legendre transformation (e.g., Ott, 1993): $\alpha(q) = \tau'(q)$, and $f(\alpha) = q\alpha - \tau$. It is well known that for $q < 0$ the spheres (or cubes) visited less frequently by a trajectory of the system are more important, and we have some basic statistical problems, as seen in Figure 2b. Nevertheless, in spite of large statistical errors in Figure 3b, especially for $q < 0$, the multifractal character of the measure can still be discerned. Therefore, one can say that the spectrum of dimensions still exhibits the multifractal structure of the slow solar wind in the inner heliosphere.

In order to quantify that multifractality, we use a simple two-dimensional analytical model of the dynamical system. Namely, we consider the generalized

self-similar baker’s map acting on the unit square with two parameters p and s describing natural invariant measure and uniform compression on the attractor of the system, correspondingly (e.g., Ott, 1993):

$$\begin{aligned} x_{n+1} &= \begin{cases} sx_n & \text{for } y_n < p \\ (1 - s) + sx_n & \text{for } y_n \geq p \end{cases} \\ y_{n+1} &= \begin{cases} \frac{y_n}{p} & \text{for } y_n < p \\ \frac{y_n - p}{1 - p} & \text{for } y_n \geq p \end{cases} \end{aligned} \tag{4}$$

where the probability of visiting one region of the square is p ($\leq 1/2$), and for the remaining region is $1 - p$. Another parameter s ($\leq 1/2$) describes both the uniform stretching and folding in the phase space, i.e., s is a folding and dissipation parameter. For the generalized dimensions of the attractor projected onto one axis, for any q in Equation (1), one obtains analytically (e.g., Ott, 1993)

$$\tau(q) \equiv (q - 1)D_q = \frac{\ln[p^q + (1 - p)^q]}{\ln s}. \tag{5}$$

The multifractal singularity spectrum $f(\alpha)$ is also obtained analytically from Equation (5) by Legendre transformation. In the absence of dissipation ($s = 1/2$) one recovers the formula for the multifractal cascade p -model for fully developed turbulence (Meneveau and Sreenivasan, 1987), which obviously corresponds to the generalized weighted Cantor set (Hentschel and Procaccia, 1983; Macek, 2002, Figure 3; Macek *et al.*, 2006, Figure 4). In particular, the usual middle one-third Cantor set without any multifractality is recovered with $p = 1/2$ and $s = 1/3$.

The difference of the maximum and minimum dimensions, associated with the least-dense and most-dense points on the attractor, correspondingly, is $D_{-\infty} - D_{+\infty} = \ln(1/p - 1)/\ln(1/s)$ and in the limit $p \rightarrow 0$ this difference rises to infinity. Hence, for a given s the parameter p can be regarded as a degree of multifractality. For illustration the results for D_q and $f(\alpha)$, fitted to the experimental values of D_q with $p = 0.12$ and $s = 0.47$ in Equation (5) (see, Macek *et al.*, 2005, Figure 3) are also shown here by dashed-dotted lines in Figure 3a and b, correspondingly. We see that the multifractal spectrum of the solar wind is roughly consistent with that for the multifractal measure on the self-similar weighted baker’s map.

Naturally, the value of the parameter p (within some factor) is related to the usual models, which starting from Richardson’s version of turbulence, try to recover the observed scaling exponents, which is based on the p -model of turbulence (e.g., Meneveau and Sreenivasan, 1987). The value of $p = 0.12$ obtained here is roughly consistent with the fitted value in the literature both for laboratory and the solar wind turbulence, which is in the range $0.13 \leq p \leq 0.3$ (e.g., Burlaga, 1991; Carbone, 1993; Carbone and Bruno, 1996; Marsch *et al.*, 1996). One should only bear in mind that here we take probability measure directly on the solar wind attractor, which quantifies multifractal nonuniformity of visiting various parts of the attractor in

the phase space, while the usual p -model is related to the solar wind turbulence cascade for the dissipation rate, which resides in the physical space.

5. Conclusions

We have shown that the multifractal spectrum of the solar wind attractor is consistent with that for the multifractal measure on the self-similar weighted baker's map. This map exhibits stretching and folding properties leading to sensitive dependence on initial conditions. The values of the parameters fitted demonstrate small dissipation of the complex solar wind plasma and show that some parts of the attractor in the phase space are visited at least one order of magnitudes more frequently than other parts (cf. Macek, 1998, Figure 5). The obtained characteristics of the attractor are significantly different from those of the surrogate data. Thus, these results show multifractal structure of the solar wind in the inner heliosphere. Hence, we suggest that there exists an inertial manifold for the solar wind, in which the system has *multifractal* structure, and where noise is certainly not dominant. The multifractal structures, convected by the wind, might probably be related to the complex topology shown by the magnetic field at the source regions of the solar wind.

Acknowledgement

This work has been supported by the Polish Ministry of Education and Science (MEiN) through Grant No. 2 P03B 126 24.

References

- Albano, A.M., Muench, J., Schwartz, C., Mees, A. I., and Rapp, P. E.: 1988, *Phys. Rev. A* **38**, 3017.
 Bruno, R., Carbone, V., Veltri, P., Pietropaolo, E., and Bavassano, B.: 2001, *Planet. Space Sci.* **49**, 1201.
 Burlaga, L.F.: 1991, *Geophys. Res. Lett.* **18**, 69.
 Burlaga, L.F.: 2001, *J. Geophys. Res.* **106**, 15917.
 Carbone, V.: 1993, *Phys. Rev. Lett.* **71**, 1546.
 Carbone, V. and Bruno, R.: 1996, *Ann. Geophys.* **14**, 777.
 Eckmann, J.-P. and Ruelle, D.: 1992, *Physica D* **56**, 185.
 Grassberger, P.: 1983, *Phys. Lett. A* **97**, 227.
 Grassberger, P. and Procaccia, I.: 1983, *Physica D* **9**, 189.
 Halsey, T. C., Jensen, M. H., Kadanoff, L. P., Procaccia, I., and Shraiman, B.I.: 1986, *Phys. Rev. A* **33**, 1141.
 Hentschel, H.G.E. and Procaccia, I.: 1983, *Physica D* **8**, 435.
 Macek, W. M.: 1998, *Physica D* **122**, 254.
 Macek, W. M.: 2002, in Boccaletti, S., Gluckman, B. J., Kurths, J., Pecora, L. M., and Spano, M. L., (eds.). *Experimental Chaos*, Vol. 622, American Institute of Physics, New York, p. 74.

- Macek, W. M.: 2003, in Velli, M., Bruno, R., and Malara, F. (eds.), *Solar Wind 10*, Vol. 679, American Institute of Physics, New York, p. 530.
- Macek, W. M., and Redaelli, S.: 2000, *Phys. Rev. E* **62**, 6496.
- Macek, W. M., Bruno, R., and Consolini, G.: 2005, *Phys. Rev. E* **72**, 017202.
- Macek, W. M., Bruno, R., and Consolini, G.: 2006, *Adv. Space Res.* **37**, 461.
- Mandelbrot, B.B.: 1989, in *Pure and Applied Geophysics*, Vol. 131, Birkhäuser Verlag, Basel, p. 5.
- Meneveau, C. and Sreenivasan, K.R.: 1987, *Phys. Rev. Lett.* **59**, 1424.
- Marsch, E. and Tu, C.-Y.: 1997, *Nonlinear Proc. Geophys.* **4**, 101.
- Marsch, E., Tu, C.-Y., and Rosenbauer, H.: 1996, *Ann. Geophys.* **14**, 259.
- Ott, E.: 1993, *Chaos in Dynamical Systems*, Cambridge University Press, Cambridge.
- Schwenn, R.: 1990, in Schwenn, R., and Marsch, E., (eds.), *Physics of the Inner Heliosphere*, Vol 20, Springer-Verlag, Berlin, p. 99.
- Theiler, J.: 1986, *Phys. Rev. A* **34**, 2427.
- Theiler, J., Eubank, S., Longtin, A., Galdrikian, B., and Farmer, J. D.: 1992, *Physica D* **58**, 77.